The Metamorphosis of Supernova SN 2008D/XRF 080109: A Link Between Supernovae and GRBs/Hypernovae

Paolo A. Mazzali, *et al.*

Science **321**, 1185 (2008);
DOI: 10.1126/science.1158088

3.5. For such a power-law distribution of electrons, the maximum degree of linear polarization that is physically possible is defined by the expression (*23*) $\Pi = (p + 1)/(p + 7/3)$ giving ~77%. Any inhomogeneities in the structure of the magnetic field will result in the degree of linear polarization being reduced. The high linear polarization measured at gamma wavelengths, roughly 60% of the maximum physical limit, implies a high degree of uniformity in the magnetic field configuration associated with the unpulsed emission and makes substantial polarized gamma-ray emission from the rather tangled magnetic field associated with the PWN unlikely.

The alignment of the polarization vector along the jet axis implies an orthogonal magnetic field configuration if the synchrotron process operates. Analyses of radio and optical polarization studies of jets in radio galaxies (*24*, *25*) indicate that the apparent magnetic field vector is parallel to the jet axis in the inner reaches of the jet, becoming perpendicular closer to the termination point. Taking the value for the magnetic field within the Crab jet close to the termination point derived from Chandra observations to be 9.1×10^{-4} G, the synchrotron process would require electrons with energies of $\sim 2 \times 10^{14}$ eV to create polarized gamma-ray photons at 400 keV and $\sim 2 \times 10^{13}$ eV for the kilo–electron volt x-rays detected by Weisskopf *et al.* (*21*).

Chandra images of the Crab (*1*) (Fig. 2) indicate that the jet is curved, so energetic electrons streaming along the jet also could radiate by curvature radiation, for which the electric vector is parallel to the jet, as observed by SPI. In the relativistic limit, the emission frequency is given by $\upsilon_c = (3c/4\pi R)\gamma^3$, where γ is the Lorentz factor of the radiating electrons and R is the radius of curvature of the field lines. Taking an estimate of $R \sim 2.5 \times 10^{18}$ cm for the Crab jet, in order to generate the few hundred kilo–electron volt photons detected by INTEGRAL, we would require electrons with energies of typically 10^{15} eV, which is entirely plausible in the context of the Crab pulsar.

The remarkable alignment of the electric vector with the rotational axis of the pulsar, together with its similarity to the optical polarization angle, suggests that both fluxes originate at the same site close to the neutron star (*26*). The higher rotation angle of the x-ray emission would suggest a different production site.

Our findings have clear implications for many aspects of high-energy accelerators, such as the production of the very high-energy (VHE) emission observed by ground-based Cerenkov detectors. A number of these tera–electron volt–emitting sources are associated with young, energetic, soft gamma-ray–emitting pulsars (*27*), including the Crab (*28*). If we assume that the VHE photons are produced by inverse Compton scattering by high-energy electrons from the pulsar on the cosmic microwave background and local starlight, there is a need for a constant supply of these electrons to be channeled from the pulsar to the extended site of the VHE emission. We have demonstrated that in the Crab, there is high-energy acceleration of electrons to at least 10^{14} to 10^{15} eV, which are then capable of producing tera–electron volt emission via inverse Compton scattering on the cosmic microwave background or some other locally produced photons.

References and Notes

1. M. C. Weisskopf *et al.*, *Astrophys. J.* **536**, L81 (2000).
2. J. J. Hester *et al.*, *Astrophys. J.* **448**, 240 (1995).
3. E. V. Gotthelf, Q. D. Wang, *Astrophys. J.* **532**, L117 (2000).
4. B. M. Gaensler, M. J. Pivovaroff, G. P. Garmire, *Astrophys. J.* **556**, L107 (2001).
5. D. J. Helfand, E. V. Gotthelf, J. P. Halpern, *Astrophys. J.* **556**, 380 (2001).
6. G. G. Pavlov, O. Y. Kargaltsev, D. Sanwal, G. P. Garmire, *Astrophys. J.* **554**, L189 (2001).
7. B. M. Gaensler *et al.*, *Astrophys. J.* **569**, 878 (2002).
8. M. S. E. Roberts *et al.*, *Astrophys. J.* **588**, 992 (2003).
9. G. G. Pavlov, M. A. Teter, O. Y. Kargaltsev, D. Sanwal, *Astrophys. J.* **591**, 1157 (2003).
10. J. J. Hester *et al.*, *Astrophys. J.* **577**, L49 (2002).
11. R. Willingale *et al.*, *Astron. Astrophys.* **365**, L212 (2001).
12. H. Mori *et al.*, *Astrophys. J.* **609**, 186 (2004).
13. M. G. F. Kirsch *et al.*, *Astron. Astrophys.* **453**, 173 (2006).
14. L. Kuiper *et al.*, *Astron. Astrophys.* **378**, 918 (2001).
15. C. Winkler *et al.*, *Astron. Astrophys.* **411**, L1 (2003).
16. A. J. Bird *et al.*, *Astrophys. J.* **170** (suppl.), 175 (2007).
17. E. Massaro, R. Campana, G. Cusumano, T. Mineo, *Astron. Astrophys.* **459**, 859 (2006).
18. S. Agostinelli *et al.*, *Nucl. Instrum. Methods Phys. Res. A* **506**, 250 (2003).
19. T. Mizuno *et al.*, *Nucl. Instrum. Methods Phys. Res. A* **540**, 158 (2005).
20. C.-Y. Ng, R. W. Romani, *Astrophys. J.* **601**, 479 (2004).
21. M. C. Weisskopf, E. H. Silver, H. L. Kestenbaum, K. S. Long, R. Novick, *Astrophys. J.* **220**, L117 (1978).
22. G. Kanbach, A. Slowikowska, S. Kellner, H. Steinle, *Am. Inst. Phys. Conf. Proc.* **801**, 306K (2005).
23. F. Lei, A. J. Dean, G. L. Hills, *Space Sci. Rev.* **82**, 309 (1997).
24. R. A. Laing, A. H. Bridle, *Mon. Not. R. Astron. Soc.* **336**, 328 (2002).
25. E. S. Perlman *et al.*, *Astrophys. J.* **651**, 735 (2006).
26. J. Takata, H.-K. Chang, K. S. Cheng, *Astrophys. J.* **656**, 1044 (2007).
27. F. Aharonian *et al.*, *Science* **307**, 1938 (2005).
28. F. Aharonian *et al.*, *Astron. Astrophys.* **457**, 899 (2006).

29. The authors thank C. Jordain and P. Dubath for supplying Crab ephemeris data and the University of Southampton for the use of their Iridis 2 Beowulf Cluster. This paper is based on observations with INTEGRAL, an ESA project with instruments and science data center funded by ESA member states (especially the principal investigator countries: Denmark, France, Germany, Italy, Switzerland, and Spain), the Czech Republic, and Poland, and with the participation of Russia and the United States. This work was supported by the Italian Space Agency with contract I/R/008/07/0 and in the United Kingdom by Science and Technology Funding Council grant PP/C000714/1.

Supporting Online Material
www.sciencemag.org/cgi/content/full/321/5893/1183/DC1
SOM Text
Figs. S1 to S5
Tables S1 and S2
References

10 August 2007; accepted 17 July 2008
10.1126/science.1149056

The Metamorphosis of Supernova SN 2008D/XRF 080109: A Link Between Supernovae and GRBs/Hypernovae

Paolo A. Mazzali,[1,2,3,4]* Stefano Valenti,[5,6] Massimo Della Valle,[7,8,9] Guido Chincarini,[10,11] Daniel N. Sauer,[1] Stefano Benetti,[2] Elena Pian,[12] Tsvi Piran,[13] Valerio D'Elia,[14] Nancy Elias-Rosa,[1] Raffaella Margutti,[10] Francesco Pasotti,[10] L. Angelo Antonelli,[14] Filomena Bufano,[2] Sergio Campana,[11] Enrico Cappellaro,[2] Stefano Covino,[11] Paolo D'Avanzo,[11] Fabrizio Fiore,[14] Dino Fugazza,[11] Roberto Gilmozzi,[8] Deborah Hunter,[5] Kate Maguire,[5] Elisabetta Maiorano,[15] Paola Marziani,[2] Nicola Masetti,[15] Felix Mirabel,[16] Hripsime Navasardyan,[2] Ken'ichi Nomoto,[3,4,17] Eliana Palazzi,[15] Andrea Pastorello,[5] Nino Panagia,[18,19] L. J. Pellizza,[20] Re'em Sari,[13] Stephen Smartt,[5] Gianpiero Tagliaferri,[11] Masaomi Tanaka,[3] Stefan Taubenberger,[1] Nozomu Tominaga,[3] Carrie Trundle,[5] Massimo Turatto[19]

The only supernovae (SNe) to show gamma-ray bursts (GRBs) or early x-ray emission thus far are overenergetic, broad-lined type Ic SNe (hypernovae, HNe). Recently, SN 2008D has shown several unusual features: (i) weak x-ray flash (XRF), (ii) an early, narrow optical peak, (iii) disappearance of the broad lines typical of SN Ic HNe, and (iv) development of helium lines as in SNe Ib. Detailed analysis shows that SN 2008D was not a normal supernova: Its explosion energy ($E \approx 6 \times 10^{51}$ erg) and ejected mass [~7 times the mass of the Sun ($M_\odot$)] are intermediate between normal SNe Ibc and HNe. We conclude that SN 2008D was originally a ~30 $M_\odot$ star. When it collapsed, a black hole formed and a weak, mildly relativistic jet was produced, which caused the XRF. SN 2008D is probably among the weakest explosions that produce relativistic jets. Inner engine activity appears to be present whenever massive stars collapse to black holes.

On 9.57 January 2008 Universal Time (UT), the x-ray telescope (XRT) on board the Swift spacecraft detected a weak x-ray flash (XRF 080109) in the galaxy NGC2770 (*1*). Optical follow-up revealed the presence of a supernova (SN) coincident with the XRF [SN 2008D; RA (2000) = 09 09 30.625; Dec (2000) = +33 08 20.16] (*2*). We detected SN 2008D photometrically from Asiago Observatory on 10.01 January 2008 UT, only 10.5 hours after the Swift detection. Early spectra showed broad absorption lines superposed on a blue continuum and lacked hydrogen or helium lines (*3*). Accordingly, SN 2008D was classified as a broad-lined SN Ic (*4*). SNe of this type are sometimes associated with gamma-ray bursts (GRBs) (*5*, *6*) or XRFs (*7*, *8*). The spectra resembled those of the XRF-SN 2006aj (*8*) or the non-GRB hypernova (HN) SN 2002ap (*9*) (Fig. 1, top), but a comparison suggests that SN 2008D was highly reddened: We estimate that $E(B-V)_{tot} = 0.65$ mag [see supporting online material (SOM)].

The host galaxy of XRF 080109/SN 2008D, NGC 2770 (redshift z = 0.006494, distance 31 Mpc), is a spiral galaxy similar to the Milky Way, M31, or ESO 184-G82, the host of SN 1998bw/GRB 980425. NGC 2770 has roughly solar metallicity and a moderate star-formation rate, ~0.5 $M_\odot$ year^{-1} (see SOM). In contrast, typical host galaxies of GRBs are small, compact, somewhat metal-poor, and highly star-forming (*10*).

In addition to the weak XRF, SN 2008D shows a number of peculiar features, most of which are new. The optical light curve had two peaks (Fig. 2): A first, dim maximum ($V \approx 18.4$) was reached less than 2 days after the XRF. After a brief decline, the luminosity increased again, reaching principal maximum (V = 17.37) ~19 days after the XRF. An 18- to 20-day risetime is typical of GRB-HNe: Normal SNe Ic reach maximum in 10 to 12 days. Few stripped-envelope SNe have very early data, and in GRB-HNe a first peak may be masked by the afterglow light. A first narrow optical peak was only seen in the type Ib SN 1999ex [SNe Ib are similar to SNe Ic but show strong helium lines (*4*)], the type IIb SN 1993J (SNe IIb are similar to SNe Ib but still have some hydrogen), and the type Ic XRF-SN 2006aj. When it was discovered, SN 1999ex was dropping from a phase of high luminosity (*11*). It reached principal maximum ~20 days later, as did SN 2008D.

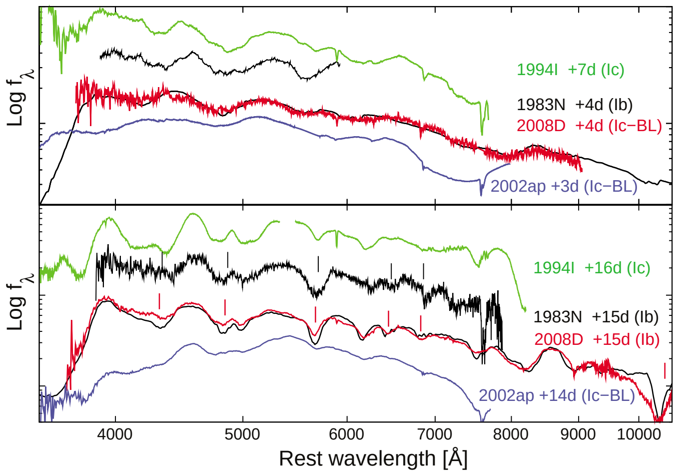

Fig. 1. The spectra of SN 2008D compared with those of other Type Ibc SNe and to simulations. Near the first peak (**top**), SN 2008D has a broad-lined spectrum similar to that of SN 2002ap, a broad-lined SN without a GRB (*9*), but different from both the normal SN Ic 1994I and the SN Ib 1983N. At the time of the main light curve peak (**bottom**), the spectrum of SN 2008D has narrow lines like SNe 1994I and 1983N, whereas SN 2002ap and other HNe retain broad features throughout their evolution. Also, SN 2008D developed He lines (vertical ticks). At this epoch, the spectra of SNe 2008D, 1983N, and 1999ex are similar. Synthetic spectra are overlaid on the two SN 2008D spectra (see SOM).

Another unusual feature is the spectral metamorphosis (Fig. 3). Unlike SNe 2006aj and 2002ap, the broad absorptions did not persist. As they disappeared, He I lines developed (*12*). By principal maximum, SN 2008D had a narrow-lined, type Ib spectrum (Fig. 1, bottom).

Broad lines require material moving with velocity $v > 0.1c$, where c is the speed of light (*13*). Their disappearance implies that the mass moving at high velocities was small.

Late development of He I lines, previously seen only in SN 2005bf (*14*), is predicted by theory (*15*). Helium levels have high excitation potentials, exceeding the energy of thermal photons and electrons. Excitation can be provided by the fast particles produced as the γ-rays emitted in the decay chain of ^{56}Ni thermalize (*16*). This is the process that makes SNe shine. In the first few days after explosion, thermalization is efficient because of the high densities and because not enough particles are available to excite helium. Only when density drops sufficiently can more particles escape the ^{56}Ni zone and excite helium.

We reproduced the spectral evolution and the light curve of SN 2008D after the first narrow peak, using a model with $M_{ej} \sim 7\ M_\odot$ and spherically symmetric $E \sim 6 \times 10^{51}$ erg, of which ~0.03 $M_\odot$, with energy ~5×10^{50} erg, are at $v >$ 0.1c (Figs. 1 and 2 and SOM). Our light curve fits indicate that SN 2008D synthesized ~0.09 $M_\odot$ of ^{56}Ni, like the non-GRB HN SN Ic 2002ap (*9*) and the normal SN Ic 1994I (*17*) but much less than the luminous GRB-HN SN 1998bw (*6*). The rapid rise in luminosity after the first peak requires that some ^{56}Ni (0.02 $M_\odot$) was mixed uniformly at all velocities > 9000 km s^{-1}. This is a typical feature of HNe and indicates an aspherical explosion (*18*). Asphericity may affect our estimate of the energy, but not the ^{56}Ni mass (*19*).

Comparing the mass of the exploding He star that we derived with evolutionary models of massive stars, we find that the progenitor had main sequence mass ~30 $M_\odot$. A star of this mass is likely to collapse to a black hole, as do GRB/SNe (*20*). So, SN 2008D shared several features of GRB/HNe. However, all SNe with GRBs or strong XRFs initially had velocities higher than SN 2008D or SN 2002ap (fig. S3) and never showed helium. Had the He layer not been present in SN 2008D, the explosion energy would have accelerated the inner core to higher velocities, and broad lines may have survived.

The characterizing features of SN 2008D (weak XRF, first narrow optical peak, initially broad-lined SN Ic spectrum that later transformed into a narrow-lined SN Ib spectrum) may be common to all SNe Ib, or at least a substantial fraction of them, and perhaps some SNe Ic (which, however, contain little or no helium). The light curves of various SNe Ib are rather similar (*21*). The first peak was observed only for SN 1999ex, but lack of x-ray monitoring probably prevented the detection of more weak XRFs and the early discovery of the associated SNe. On the other hand, SN 2008D (and possibly most SNe Ib) was more energetic than normal core-collapse SNe, including most SNe Ic.

Type II SNe in late spiral/irregular galaxies (the typical Hubble type of GRB hosts) are about 6 times as frequent as SNe Ib (*22*). Although the serendipitous discovery of an SN Ib by XRT may be a statistical fluctuation, it may also suggest that the soft x-ray emission accompanying SN 2008D is typical of overenergetic SNe Ib and absent (or very weak) in normal core-collapse SNe.

The x-ray spectrum of SN 2008D (in total ~500 photons) can be fitted with either a simple

[1]Max-Planck Institut für Astrophysik, Karl-Schwarzschild-Strasse 1, 85748 Garching, Germany. [2]Istituto Nazionale di Astrofisica-OAPd, vicolo dell'Osservatorio, 2, I-35122 Padova, Italy. [3]Department of Astronomy, School of Science, University of Tokyo, Bunkyo-ku, Tokyo 113-0033, Japan. [4]Research Center for the Early Universe, School of Science, University of Tokyo, Bunkyo-ku, Tokyo 113-0033, Japan. [5]Astrophysics Research Centre, School of Mathematics and Physics, Queen's University, Belfast, BT7 1NN, Northern Ireland, UK. [6]Dipartimento di Fisica, Universita di Ferrara, Via Giuseppe Saragat 1, 44100 Ferrara, Italy. [7]Istituto Nazionale di Astrofisica, Capodimonte Astronomical Observatory, Salita Moiariello 16, I-80131 Napoli, Italy. [8]European Southern Observatory, Karl-Schwarzschild-Strasse 2, D-85748 Garching, Germany. [9]International Center for Relativistic Astrophysics Network, Piazzale della Repubblica 10, I-65122 Pescara, Italy. [10]Department of Physics, Universita di Milano-Bicocca, Piazza delle Scienze 3, I-20126 Milano, Italy. [11]Istituto Nazionale di Astrofisica, Brera Astronomical Observatory, Via Emilio Bianchi 46, I-23807 Merate (LC), Italy. [12]Istituto Nazionale di Astrofisica-OATs, Via Tiepolo 11, I-34131 Trieste, Italy. [13]The Racah Institute of Physics, Hebrew University, Jerusalem 91904, Israel. [14]Istituto Nazionale di Astrofisica, Rome Astronomical Observatory, Via di Frascati 33, I-00040 Monte Porzio Catone, Italy. [15]Istituto Nazionale di Astrofisica, Istituto di Astrofisica Spaziale e Fisica Cosmica, Via Piero Gobetti 101, I-40129 Bologna, Italy. [16]European Southern Observatory, Alonso de Cordova 3107, Santiago, Chile. [17]Institute for the Physics and Mathematics of the Universe, University of Tokyo, Kashiwa, Chiba 277-8582, Japan. [18]Space Telescope Science Institute, 3700 San Martin Drive, Baltimore, MD 21218, USA. [19]Istituto Nazionale di Astrofisica, Catania Astronomical Observatory, Via Santa Sofia 78, I-95123 Catania, Italy. [20]Instituto de Astronomía y Física del Espacio, Casilla de Correos 67, Buenos Aires, Argentina.

*To whom correspondence should be addressed. E-mail: mazzali@mpa-garching.mpg.de

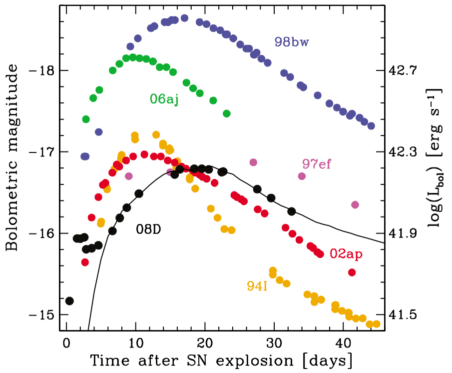

Fig. 2. The light curves of SN 2008D and of other type Ibc SNe. The shape of the light curve of SN 2008D is similar to that of SN 1998bw and other GRB/HNe, and comparable to the non-GRB HN SN 1997ef, but much broader than the XRF/SN 2006aj or the normal SN Ic 1994I. This similarity suggests a comparable value of the quantity M_{ej}^3 / E, where M_{ej} is the mass ejected and E the explosion kinetic energy (*28*). All known SNe Ic with a broad light curve ejected a large mass of material (*29*). Large values of M_{ej} and E are also suggested by the presence of He moving at $v \sim 10{,}000$ km s^{-1}: The velocity of He in SN 2005bf was lower (*14*). The light curve of SN 1999ex, which is similar to that of SN 2008D, was fitted reasonably well by a He-star explosion model with $M_{ej} \sim 5\ M_\odot$ and $E \sim 3 \times 10^{51}$ erg (*11*). Such a model would also match the light curve of SN 2008D, but it probably would not reproduce the broad lines that characterize the early spectra. This would require a model containing some high-velocity material, leading to a larger E without noticeably affecting the value of M_{ej} or the light curve shape. The line shows a synthetic bolometric light curve computed with a Monte Carlo code (*30*) for a model with $M_{ej} \sim 7\ M_\odot$ and $E \sim 6 \times 10^{51}$ erg. The model does not address the physics that may be responsible for the first narrow light curve peak, but only the main peak, which is due to diffusion of radiation in the SN envelope following the deposition of γ-rays and positrons emitted in the decay chain ^{56}Ni to ^{56}Co and ^{56}Fe.

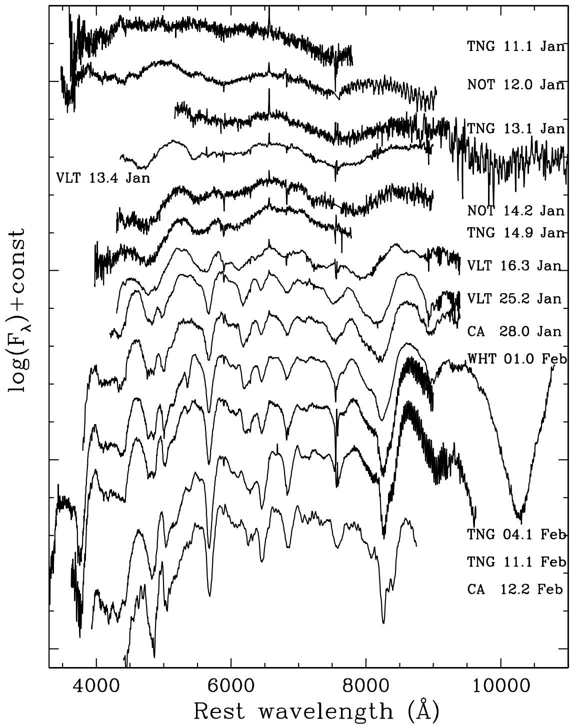

Fig. 3. Spectral evolution of SN 2008D. In the early phase, the strongest features are broad Fe complexes in the blue (~4000 to 5000 Å), the Si II-dominated feature near 6000Å, and Ca II lines, both in the near ultraviolet (H and K) and in the near infrared (the infrared triplet near 8500 Å). On the other hand, O I 7774 Å, which is strong in all HNe as well as in all SNe Ibc, is conspicuously missing. Starting 15 January, lines begin to become narrow. In the later spectra, taken near maximum, He I lines have developed. The strongest isolated lines are λ6678 Å, seen near 6500 Å, and λ7065 Å, seen near 6900 Å. Both lines indicate a helium velocity of ~10,000 km s^{-1}. The other strong optical lines of He I are blended: λ5876 Å is blended with Na I D, near 5600 Å, and λ4471 Å is blended with the broad Fe II trough near 4200 Å.

power law indicating a nonthermal emission mechanism or a combination of a hot black body ($T = 3.8 \times 10^6$ K) and a power law. In the latter case, the unabsorbed luminosity of the black-body component is a small fraction of the total x-ray luminosity. The high temperature and low luminosity ($L = 1.1 \times 10^{43}$ erg s^{-1}) of the black-body component at first peak (~100 s after the onset of the XRF) imply an emitting radius $R_{ph} \sim 10^{10}$ cm (see SOM, Section 4). This is at least one order of magnitude smaller than the size of Wolf-Rayet stars, the likely progenitors of SNe Ibc.

The x-ray flare and the first optical peak are most likely associated (*23*). The time scale of the first optical peak may suggest that it was related to shock breakout. A signature of shock breakout is a hot black-body x-ray spectrum immediately after the explosion. Thermal x-ray emission was suggested for SN 2006aj (*24*), whereas no x-ray data are available for SN 1999ex. The model of (*23*) uses a spherical configuration and a black-body component at ~0.1 keV, below the XRT energy range. This yields a large radius, which the authors explain by invoking the presence of a dense surrounding medium that bulk-Comptonizes the shock breakout emission to higher energies, producing the power-law spectrum observed by XRT between 0.3 and 10 keV.

On the other hand, the angular size of an emitting area with radius $R_{ph} \sim 10^{10}$ cm is typical of GRB jets. This leads naturally to an alternative scenario, which we propose here: XRF 080109 was the breakout of a failed relativistic jet powered by a central engine, as in GRBs. The jet failed because its energy was initially low or because it was damped by the He layer, which is absent in GRB-HNe, or both. The presence of a jet is supported by our conclusions that SN 2008D was highly energetic and that a black hole was probably formed when the star collapsed. The marginal breakout of the jet produced thermal x-rays and relativistic particles that caused the power-law x-ray component. It also caused the first optical peak: The time scale of the first peak and the x-ray flare and the corresponding radii and temperature are consistent with emission from rapidly expanding, adiabatically cooling material. The weakness of the jet resulted in the low x-ray flux and the small amount of material with $v > 0.1c$. The failed jet contributed anisotropically to the SN kinetic energy. Lateral spreading of the ejecta with $v > 0.1c$ leads to an angular size larger than the x-ray–emitting region, which is needed to produce the observed broad lines. The small amount of high-velocity material moving along our line of sight may also indicate that we viewed the explosion considerably off-axis. This can be tested by polarization or line profile studies at late times, as in SN 2003jd (*25*). The jet will spread further after breakout, and it could dominate the radio emission at later times.

The scenario we propose implies that GRB-like inner engine activity exists in all black hole–forming SNe Ibc (*26*). SN 2008D (and probably other SNe Ib) has significantly higher energy than normal core-collapse SNe, although less than GRB/HNe. Therefore, it is unlikely that all SNe Ibc, and even more so all core-collapse SNe, produce a weak x-ray flash similar to XRF 080109. The presence of high-energy emission (GRB or XRF) depends on the jet energy and the stellar properties. Only massive, energetic, stripped SNe Ic (HNe) have shown GRBs. In borderline events like SN 2008D, only a weak, mildly relativistic jet may emerge, because the collapsing mass is too small and a He layer damps the jet. For even less massive stars that still collapse to a black hole, producing a less energetic explosion (e.g., SN 2002ap), no jet may emerge at all. Stars that only collapse to a neutron star are not expected to have jets unless the neutron star is rapidly spinning (*27*). SN 2008D thus links events that are physically related but have different observational properties.

References

1. E. Berger, A. M. Soderberg, GCN 7159 (2008); http://gcn.gsfc.nasa.gov/gcn3/7159.gcn3.
2. J. Deng, Y. Zhu, GCN 7160 (2008); http://gcn.gsfc.nasa.gov/gcn3/7160.gcn3.
3. S. Valenti *et al.*, GCN 7171 (2008); http://gcn.gsfc.nasa.gov/gcn3/7171.gcn3.
4. A. V. Filippenko, *Annu. Rev. Astron. Astrophys.* **35**, 309 (1997).
5. T. J. Galama *et al.*, *Nature* **395**, 670 (1998).
6. K. Iwamoto *et al.*, *Nature* **395**, 672 (1998).
7. E. Pian *et al.*, *Nature* **442**, 1011 (2006).
8. P. A. Mazzali *et al.*, *Nature* **442**, 1018 (2006).

9. P. A. Mazzali *et al.*, *Astrophys. J.* **572**, L61 (2002).
10. A. S. Fruchter *et al.*, *Nature* **441**, 463 (2006).
11. M. Stritzinger *et al.*, *Astron. J.* **124**, 2100 (2002).
12. M. Modjaz, R. Chornock, R. J. Foley, A. V. Filippenko, W. Li, G. Stringfellow, GCN 7212 (2008); http://gcn.gsfc.nasa.gov/gcn3/7212.gcn3.
13. P. A. Mazzali, K. Iwamoto, K. Nomoto, *Astrophys. J.* **545**, 407 (2000).
14. N. Tominaga *et al.*, *Astrophys. J.* **633**, L97 (2005).
15. P. A. Mazzali, L. B. Lucy, *Mon. Not. R. Astron. Soc.* **295**, 428 (1998).
16. L. B. Lucy, *Astrophys. J.* **383**, 308 (1991).
17. D. Sauer *et al.*, *Mon. Not. R. Astron. Soc.* **369**, 1939 (2006).
18. K. Maeda *et al.*, *Astrophys. J.* **593**, 931 (2003).
19. K. Maeda, P. A. Mazzali, K. Nomoto, *Astrophys. J.* **645**, 1331 (2006).
20. A. E. MacFadyen, S. E. Woosley, *Astrophys. J.* **524**, 262 (1999).
21. A. Clocchiatti, J. C. Wheeler, *Astrophys. J.* **491**, 375 (1997).
22. E. Cappellaro, R. Evans, M. Turatto, *Astron. Astrophys.* **351**, 459 (1999).
23. A. M. Soderberg *et al.*, *Nature* **453**, 469 (2008).
24. S. Campana *et al.*, *Nature* **442**, 1008 (2006).
25. P. A. Mazzali *et al.*, *Science* **308**, 1284 (2005).
26. K. Maeda *et al.*, *Science* **319**, 1220 (2008).
27. N. Bucciantini *et al.*, *Mon. Not. R. Astron. Soc.* **383**, L2 (2008).
28. W. D. Arnett, *Astrophys. J.* **253**, 785 (1982).
29. P. A. Mazzali *et al.*, *Astrophys. J.* **645**, 1323 (2006).
30. E. Cappellaro *et al.*, *Astron. Astrophys.* **328**, 203 (1997).

Supporting Online Material
www.sciencemag.org/cgi/content/full/1158088/DC1
Methods
SOM Text
Figs. S1 to S4
Tables S1 and S2
References

20 March 2008; accepted 10 July 2008
Published online 24 July 2008;
10.1126/science.1158088
Include this information when citing this paper.

Hydrodefluorination of Perfluoroalkyl Groups Using Silylium-Carborane Catalysts

Christos Douvris and Oleg V. Ozerov*

Carbon-fluorine bonds are among the most unreactive functionalities in chemistry. Interest in their activation arises in part from the high global warming potentials of anthropogenic polyfluoroorganic compounds. Conversion to carbon-hydrogen bonds (hydrodefluorination) is the simplest modification of carbon-fluorine bonds, but efficient catalytic hydrodefluorination of perfluoroalkyl groups has been an unmet challenge. We report a class of carborane-supported, highly electrophilic silylium compounds that act as long-lived catalysts for hydrodefluorination of trifluoromethyl and nonafluorobutyl groups by widely accessible silanes under mild conditions. The reactions are completely selective for aliphatic carbon-fluorine bonds in preference to aromatic carbon-fluorine bonds.

Carbon-fluorine bonds are among the most passive functionalities in chemistry (*1*), and their selective activation and transformation under mild conditions remains a poorly realized challenge (*2*–*5*). The thermodynamic issues are considerable: C-F is the strongest single bond to carbon (*1*–*3*). The thermodynamic obstacles are compounded by the kinetic issues: Organic fluorides are poor ligands or Lewis bases, and poor substrates for nucleophilic substitution or oxidative addition to metals (*1*–*4*). In all of these regards, compounds containing fully fluorinated perfluoroalkyl groups prove even more inert than compounds containing a single C-F bond. With the increasing degree of fluorination at carbon, the strength of the C-F bond increases, and the C-F bond distances decrease, resulting in substantial steric shielding of the carbon site (*3*).

Perfluoroalkyl-containing organic compounds have beneficial uses in technology. Some applications include blood substitutes fostered by high O_2 solubility and inertness, (*1*, *6*) as well as solvent media for biphasic synthesis and purification (fostered by low miscibility with water and hydrocarbons) (*6*). On the other hand, perfluorooctanesulfonic acid derivatives (PFOS), used in surfactants and in fluorinated polymer production, have been recently shown to be toxic, widely spread in the biota, and highly persistent (*7*). Perfluoroalkyl-containing chlorofluorocarbons (freons or CFC), hydrofluorocarbons (partially fluorinated alkanes, HFC) and perfluorocarbons (perfluoroalkanes, PFC) are of increasing concern as anthropogenic "super-greenhouse gases" (*8*) of high global warming potential and exceedingly high atmospheric lifetimes. Development of efficient and economical chemical strategies for their disposal is thus of vital importance.

Transition-metal–mediated C-F activation has received substantial attention (*2*–*5*). The approach typically employs highly reducing, electron-rich metal reagents or catalysts. The critical cleavage of the C-F bond in this case is by definition of reductive nature, either through an oxidative addition or a single-electron transfer step. The simplest modification of the C-F bond is its conversion to the simplest functional group: a C-H bond (hydrodefluorination or HDF). The scope of the transition metal–catalyzed HDF has been largely limited to fluoroarenes (*2*–*5*). HDF of poly(tetrafluoroethylene) by stoichiometric Li metal in ammonia has been reported (*9*). Conversion of a C-F to a C-C bond is also of interest, but the progress so far has been limited (*10*). Recently, a Nb-mediated activation of trifluoromethylarene substrates with concomitant conversion of C-F bonds to C-H and C-C bonds was reported (*11*).

We were attracted to a conceptually different approach to C-F activation, in which the key C-F cleavage proceeds by a Lewis acid abstraction of fluoride rather than a redox event (Fig. 1A). Conventional acids, such as SiO_2 or concentrated H_2SO_4, require very high temperatures for cleavage of C-F bonds in perfluoroalkyl groups (*12*, *13*). In 2005, we reported an implementation of the nonredox approach under ambient conditions by using a silylium (R_3Si^+) Lewis acid (*14*). The proposed mechanism is depicted in Fig. 1A. Abstraction of fluoride by silylium from a C-F bond is complemented by the abstraction of hydride by the resultant carbocation from an Si-H bond. The overall process can be viewed as a Si-H/C-F metathesis (with conversion to Si-F/C-H). Given that Si-F is a stronger bond than C-F, and C-H is a stronger bond than Si-H, this metathesis is a very

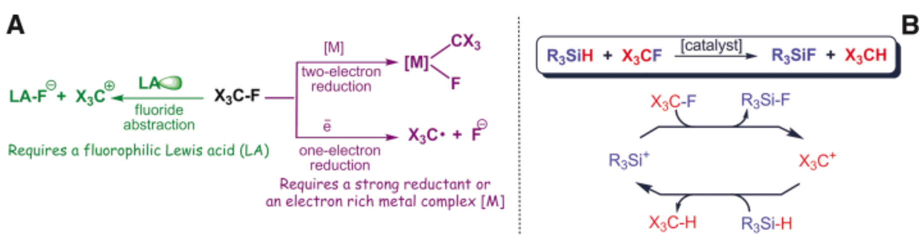

Fig. 1. (**A**) Representation of different approaches to C-F bond cleavage. X stands for an organic substituent, and the X_3 notation does not imply that the three substituents must be identical. (**B**) The stoichiometry of Si-mediated HDF and the proposed mechanism.

Department of Chemistry, Brandeis University, MS 015, 415 South Street, Waltham, MA 02454, USA.

*To whom correspondence should be addressed. E-mail: ozerov@brandeis.edu